Journal of Orthopaedic Translation 39 (2023) 135–146

Contents lists available at ScienceDirect

Journal of Orthopaedic Translation

journal homepage: www.journals.elsevier.com/journal-of-orthopaedic-translation

Original Article

Pharmacological network analysis of the functions and mechanism of kaempferol from Du Zhong in intervertebral disc degeneration (IDD)

Xiaobin Wang [a,1], Yanlin Tan [b,1], Fusheng Liu [a], Jingyu Wang [a], Fubin Liu [a], Qianshi Zhang [a], Jing Li [a,*]

[a] Department of Spine Surgery, Spinal Deformity Center, The Second Xiangya Hospital of Central South University, Changsha, Hunan, 410011, China
[b] PET/CT Center, The Second Xiangya Hospital of Central South University, Changsha, Hunan, 410011, China

ARTICLE INFO

Keywords:
Eucommia ulmoides Oliver (du zhong DZ)
Kaempferol
Intervertebral disc degeneration (IDD)
Nucleus pulposus cell (NPC)
Network pharmacology

ABSTRACT

Background: Senescence and apoptosis of the nucleus pulposus cells (NPCs) are essential components of the intervertebral disc degeneration (IDD) process. Senescence and anti-apoptosis treatments could be effective ways to delay or even stop disc degeneration. IDD has been treated with *Eucommia ulmoides* Oliver (Du Zhong, DZ) and its active ingredients. However, the roles and mechanisms of DZ in NPC apoptosis and senescence remain unclear.
Methods: Traditional Chinese Medicine Systems Pharmacology (TCMSP) database was used to select the main active ingredients of DZ with the threshold of oral bioavailability (OB) $\geq$ 30% and drug-likeness (DL) $\geq$ 0.2. GSE34095 contained expression profile of degenerative intervertebral disc tissues and non-degenerative intervertebral disc tissues were downloaded for different expression genes analysis. The disease targets genes of IDD were retrieved from GeneCards. The online tool Metascape was used for functional enrichment annotation analysis. The specific effects of the ingredient on IL-1β treated NPC cell proliferation, cell senescence, reactive oxygen species (ROS) accumulation and cell apoptosis were determined by CCK-8, SA-β-gal staining, flowcytometry and western blot assays.
Results: A total of 8 active compounds of DZ were found to meet the threshold of OB $\geq$ 30% and DL $\geq$ 0.2 with 4151 drug targets. After the intersection of 879 IDD disease targets obtained from GeneCards and 230 DEGs obtained from the IDD-related GSE dataset, a total of 13 hub genes overlapped. According to functional enrichment annotation analysis by Metascape, these genes showed to be dramatically enriched in AGE-RAGE signaling, proteoglycans in cancer, wound healing, transmembrane receptor protein tyrosine kinase signaling, MAPK cascades, ERK1/2 cascades, PI3K/Akt signaling pathway, skeletal system, etc. Disease association analysis by DisGeNET indicated that these genes were significantly associated with IDD, intervertebral disc disease, skeletal dysplasia, and other diseases. Active ingredients-targets-signaling pathway networks were constructed by Cytoscape, and kaempferol was identified as the hub active compound of DZ. In the IL-1β-induced IDD *in vitro* model, kaempferol treatment significantly improved IL-1β-induced NPC cell viability suppression and senescence. In addition, kaempferol treatment significantly attenuated IL-1β-induced ROS accumulation and apoptosis. Furthermore, kaempferol treatment partially eliminated IL-1β-induced decreases in aggrecan, collagen II, SOX9, and FN1 levels and increases in MMP3, MMP13, ADAMTS-4, and ADAMTS-5. Moreover, kaempferol treatment significantly relieved the promotive effects of IL-1β stimulation upon p38, JNK, and ERK1/2 phosphorylation. ERK1/2 inhibitor PD0325901 further enhanced the effect of kaempferol on the inhibition of ERK1/2 phosphorylation, downregulation of MMP3 and ADAMTS-4 expression, and upregulation of aggrecan and collagen II expressions.
Conclusion: Kaempferol has been regarded as the major active compound of DZ, protecting NPCs from IL-1β-induced damages through promoting cell viability, inhibiting cell senescence and apoptosis, increasing ECM production, and decreasing ECM degradation. MAPK signaling pathway may be involved.

* Corresponding author.
E-mail address: jingli1969@csu.edu.cn (J. Li).
[1] The authors contribute equally to this study

https://doi.org/10.1016/j.jot.2023.01.002
Received 18 March 2022; Received in revised form 21 December 2022; Accepted 5 January 2023

The translational poteintial of this article: This study provides *in vitro* experimental data support for the pharmacological effects of kaempferol in treating IDD, and lays a solid experimental foundation for its future clinical application in IDD treatment.

1. Introduction

Intervertebral disc degeneration (IDD) is a key contributor to lower back pain and strains healthcare systems worldwide [1]. The intervertebral disc (IVD) serves as a flexible cushion between the two vertebrae that aids in load-carrying and shock absorption. It is composed of an outer cartilaginous ring called the annulus fibrosus (AF), and an inner gelatinous core called the nucleus pulposus (NP) [2]. NP cells, which are found in the disc's inner core, are responsible for constructing and maintaining the extracellular matrix (ECM). The widespread consensus is that NP cell depletion and ECM degradation trigger the development of IDD [3]. During the IDD process, IL-1β has been reported to significantly increase in the IDD tissues. IL-1β is involved in multiple pathological processes, including matrix destruction, cellular apoptosis, oxidative stress, and cellular senescence [4]. Therefore, inhibiting IL-1β-induced NP cell apoptosis and senescence in the process of IDD may be a useful method to prevent or even reverse disc degeneration.

The degenerative state of the intervertebral disc is referred to as a "stagnation syndrome" in Traditional Chinese Medicine (TCM) [5]. Its prevalence is vulnerable to 'Damp (shi)' and 'Cold (han)' and directly associated with renal function [6]. There are presently two clinical therapeutic options available to treat IDD: surgical and non-surgical methods. The cost of surgical treatment comes with some surgical risk, and the reoperation rate ranges from 6% to 24% [7,8]. TCM has been used in non-surgical therapy in China and other Asian countries for thousands of years. It has the specific advantages of being secure, efficient, and incurring fewer adverse effects [9]. According to TCM theory and the compatibility guideline, the prescription may be treated with several concepts, multiple targets, and multiple approaches with the goals of kidney tonifying, expelling wind, removing moisture, and eliminating stasis. Reportedly, active compounds from Dan Shen (*Salvia miltiorrhiza* Bunge) [10], Lei Gong Teng (*Tripterygium wilfordii* Hook F) [6], and Du Zhong (*Eucommia ulmoides* Oliver) [11] have been used for IDD treatment. The underlying mechanism of the TCM active compounds against IDD has not yet been fully elucidated.

Through integrated bioinformatics analysis, network-based pharmacological techniques may comprehensively reflect and reveal the biological underpinnings of complex disorders and have thus emerged as a fresh and popular analytical paradigm [12]. Interestingly, the large majority of TCM and global ethnomedicine target different molecules in the human body to provide therapeutic benefits [13]. As a result, a comprehensive method of network-based pharmacology in TCM research may be a highly effective new method for locating possible treatment targets for IDD. Herein, we retrieved the main active compounds of DZ from the Traditional Chinese Medicine System Pharmacology (TCMSP) Database (http://lsp.nwu.edu.cn/tcmsp.php) [14], analyzed the targets of the main active compounds and IDD, as well as differentially expressed genes (DEGs) between IDD samples and normal control, and compared drug targets, disease targets, and DEGs. For functional enrichment annotation and disease association analysis, overlapping hub genes were used. Networks of active components, targets, and signaling pathways were built, kaempferol was chosen for additional testing, and the specific effects of kaempferol on IL-1β-simulated human nucleus pulposus cells (NPCs) were subsequently examined.

2. Materials and methods

2.1. DZ active compounds retrieved from the Traditional Chinese Medicine System Pharmacology (TCMSP) Database

The active ingredients of DZ were collected from TCMSP (http://lsp.nwu.edu.cn/tcmsp.php) [14]. Active compounds' information retrieval was performed based on ADME (absorption, distribution, metabolism, and excretion) using pharmacokinetic information retrieval filters. The thresholds of the screening conditions were oral bioavailability (OB) $\geq$ 30% and drug-likeness (DL) $\geq$ 0.2 [15].

2.2. Compounds targets and disease target retrieval

The drug targets of the active ingredients in DZ were obtained from the PubChem database (https://pubchem.ncbi.nlm.nih.gov/). Using Gene Cards, a search for the term "intervertebral disc degeneration" yielded the disease target genes of IDD.

2.3. Differentially expressed genes between SCI and normal samples

GSE34095 was downloaded from Gene Expression Omnibus (GEO) datasets (https://www.ncbi.nlm.nih.gov/geo/query/acc.cgi?acc=GSE34095) contains DEGs between human intervertebral disc tissues from older patients with degenerative disc disease (degenerative specimen, n = 3) and younger individuals with adolescent idiopathic scoliosis (considered as the normal intervertebral disc tissues specimen, n = 3) [16]. RNA extraction and hybridization were performed on the Affymetrix Human Genome U133A array. A total of 22,283 genes were identified. DEGs between degenerative disc specimens and normal intervertebral disc specimens were identified via GEO2R online tools [17] with $|\log FC| > 0.3$ and adjusted P value < 0.05. Following comparisons of DEGs, drug targets, and disease targets, 13 overlapping genes were chosen for the subsequent experiments. The principal component analysis (PCA) was performed by Python (version3.7.8).

2.4. Gene ontology (GO) functional enrichment annotation on 13 overlapped genes

The functional annotation tool of Metascape (https://metascape.org/gp/) was used to conduct the GO functional enrichment annotation [18] and Kyoto Encyclopedia of Genes and Genomes (KEGG) enrichment analysis. Terms with the default threshold were selected in functional annotation clustering. R language ggplot2 package was used for drawing the GO and KEGG bubble charts. The disease association analysis was performed based on DisGeNET (https://www.disgenet.org/) [19].

2.5. Construction and analysis of networks

The ingredient-target-pathway networks were constructed using Cytoscape_v3.8.0 [20]. The nodes in the graphical networks represented the components, proteins, or routes, and the edges of the interactions between the components and their targets or pathways.

2.6. Cell lineage, cell culture, and cell treatment

Human nucleus pulposus cells (NPCs) were procured from Procell (Catalog CP-H097; Wuhan, China) and cultivated in DMEM/F12 medium containing 15% fetal bovine serum (FBS, Gibco, Waltham, MA, USA). NPCs were cultivated at 37 °C in a humidified atmosphere containing 5% CO_2. The toluidine blue staining was used for the identification of NPCs as previous description [21]. For the *in vitro* IDD model, NPCs were treated with IL-1β (10 ng/ml, Sino Biological, China) for 24 h. For the ERK1/2 pathway inhibitor, NPCs cells were treated with PD0325901 (1 μM, Beyotime, China) for 24 h.

2.7. Immunofluorescent (IF) staining

Cells were washed thrice in PBS before being fixed in 4% paraformaldehyde for 15 min and rinsed in PBS, followed by incubation for 20 min in 0.5% Triton X-100 at ambient temperature before being rinsed in PBS. Dropwise additions of bovine serum albumin (5%) were used to the Petri dishes, followed by incubation for 30 min at ambient temperature. Cells were then incubated with ani-aggrecan (13880-1-AP, Proteintech, Wuhan, China) at 4 °C overnight, rinsed, incubated at 37 °C for 30 min in the buffer of goat anti-rabbit IgG conjugated to FITC at dark, washed in PBS, stained with 6-diamidino-2-phenylindole (DAPI), mounted with 50% glycerine, and determined using a fluorescence microscope (Olympus).

2.8. CCK-8

Cells were plated onto a 96-well plate at a density of 10^4 cells/well, with a medium volume of 100 μl. After 48 h of culture, 10 μl CCK8 solution was added to each well. Following another 2 h of incubation, the absorbance value (OD) of each well at 450 nm was measured using a Microplate reader.

2.9. β-Gal senescence staining

Cells were plated into a 6-well plate and rinsed twice in PBS buffer. After being fixed with 0.2% glutaraldehyde for 10 min at room temperature, cells were rinsed twice in PBS buffer before being stained in an X-gal staining solution overnight [22]. SA-β-gal positive cells were counted in 6 randomly selected images and the percentages of SA-β-gal positive cells were averaged for statistical analysis using an inverted microscope (Olympus).

2.10. Flow cytometry assay

An assay kit for measuring reactive oxygen species (ROS) in cells was used (Beyotime, China). Cell suspensions were, in essence, treated with 10 μM DCFH-DA for 20 min at 37 °C. The cells were subjected to flow cytometry analysis after being washed thrice with PBS. According to the manufacturer's instructions, the FITC-Annexin V/PI apoptosis detection kit (Keygen Biotech, China) was used to identify cell apoptosis. Briefly, 195 μl cell suspension (5×10^5 cells) were incubated with 5 μl FITC-Annexin V and 10 μl PI at room temperature for 15 min at dark. Then, cells underwent flow cytometry analysis (BD, USA).

2.11. qRT-PCR analysis

The total RNA from NPCs was isolated by TRIzol (invitrogen). cDNA was synthesized by The PrimeScript RT reagent Kit (Takara, Japan). Real-time PCR was performed by RealStar Fast SYBR qPCR mix with a real-time thermal cycler (AnalytikJena, German), and GAPDH was considered as endogenous control. The relative mRNA was calculated using the $2^{-\Delta\Delta Ct}$ method [23]. The primer sequence is listed in Table S1.

2.12. Immunoblotting

The following primary antibodies were used in this study: p16 (CSB-PA003618, CUSABIO, Wuhan, China), p21 (ab109520, Abcam, Cambridge, UK), Rb (ab224426, Abcam), hTERT (DF7129, Affinity Biotech), Nrf2 (CSB-RA225569A0HU,Cusabio), HO-1 (10701-1-AP, Proteintech), NQO-1 (11451-1-AP, Proteintech), SOD1 (10269-1-AP, Proteintech), SOD2 (ab227091, Abcam), Cleaved-caspase 3 (ab2302, Abcam), Caspase 3 (ab13847, Abcam), Bax (50599-2-Ig, Proteintech), Bcl-2 (12789-1-AP, Proteintech), aggrecan (13880-1-AP, Proteintech), collagen II (CSB-PA005739ESR2HU, Cusabio), SOX9 (ab185966, Abcam), FN1 (AF5335, Affinity Biotech), MMP2 (CSB-PA003258, Cusabio), MMP3 (17873-1-AP, Proteintech), MMP13 (CSB-PA07029A0Rb, Cusabio), ADAMTS-4 (DF6986, Affinity Biotech), ADAMTS-5 (DF13268, Affinity Biotech), p-p38 (AF4001, Affinity Biotech), p38 (14064-1-AP, Proteintech), p-JNK (AF3318, Affinity Biotech), JNK (AF6319, Affinity Biotech), p-ERK1/2 (sc-81492, Santa Cruz, Dallas, DX, USA), ERK1/2 (16443-1-AP, Proteintech).

Target cells were sonicated to lyse in ice-cold RIPA buffer. Total proteins were extracted from the extract using centrifugation. A BCA protein assay kit was used to measure the protein level (Beyotime, China). The denatured protein was then placed into SDS-PAGE to be separated after that. Separated proteins were then transferred to PVDF membranes and incubated with the primary antibodies listed above at 4 °C overnight. After being washed, the membranes were then incubated with goat anti-rabbit or mouse IgG buffer conjugated to HRP for 2 h at room temperature. The membranes were then activated with an enhanced chemiluminescence substrate and examined with an automatic chemiluminescence image system (Tannon-5200, China).

2.13. Statistical analysis

All data are exhibited as means ± standard deviation (SD) of at least three independent experiments. SPSS v.18.0 software (SPSS, Chicago, IL, USA) was employed to process data. Student's *t*-test or one-way analysis of variance (ANOVA) followed by Tukey's test were performed to evaluate the difference between the means of the two groups. $P < 0.05$ was deemed as a statistically significant difference.

3. Results

3.1. Drug targets of E. ulmoides oliver (du Zhong, DZ) active compounds and disease targets of interverbal disc degeneration (IDD)

Firstly, the active ingredients of DZ were retrieved from TCMSP; among all active compounds, 8 of them met the thresholds of OB ≥ 30% and DL ≥ 0.2 (Table 1). The drug targets of the active ingredients in DZ were collected from the PubChem database (https://pubchem.ncbi.nlm.nih.gov/) and a total of 4151 drug targets were obtained. The disease target genes of IDD were obtained by searching the keyword 'intervertebral disc degeneration' based on Gene Cards, and a total of 879 disease targets were obtained. DEGs between IDD tissues and normal IVD tissues were first analyzed based on GSE34095; a total of 230 DEGs with |logFC|> 0.3 and $P < 0.05$ (Fig. 1A). For identifying DZ drug targets and IDD disease

Table 1
Active compounds of *Eucommia ulmoides* Oliver (Du Zhong, DZ).

Compound	MW	OB (%)	DL	Target
ent-Epicatechin	290.29	48.95984114	0.24162	1
beta-sitosterol	414.79	36.91390583	0.75123	1
Cyclopamine	411.69	55.42172002	0.82136	79
Acanthoside B	580.64	43.35308428	0.76689	11
quercetin	302.25	46.43334812	0.27525	3980
beta-carotene	536.96	37.18433337	0.58358	183
kaempferol	286.25	41.88224954	0.24066	193
Mairin	456.78	55.37707338	0.7761	57

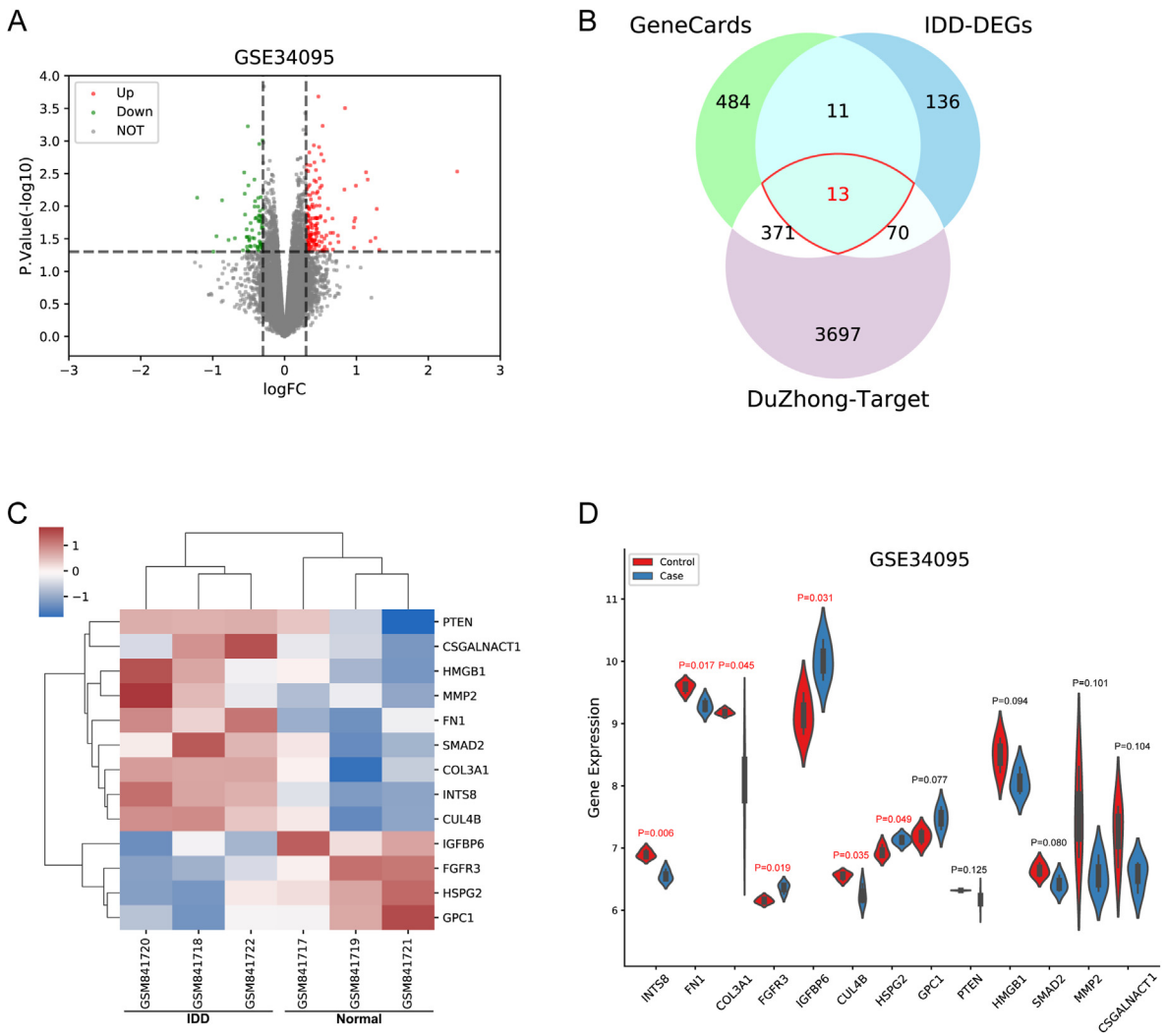

Fig 1. Drug targets of *Eucommia ulmoides* Oliver (Du Zhong, DZ) active compounds and disease targets of interverbal disc degeneration (IDD) (A) Differentially expressed genes (DEGs) between human intervertebral disc tissues from elderly patients with degenerative disc disease and younger patients with adolescent idiopathic scoliosis, respectively, based on GSE34095 (B) The drug targets of the active compounds in DZ were obtained from the PubChem database (https://pubchem.ncbi.nlm.nih.gov/). The disease target genes of IDD were obtained through searching the keyword 'intervertebral disc degeneration' based on Gene Cards. Drug targets, disease targets, and DEGs were compared and 13 overlapped genes were selected for the following analysis (C–D) The expression of these 13 genes in IDD and control samples according to GSE34095.

targets, drug targets, disease targets, and DEGs were compared and 13 overlapped genes (INTS8, FN1, COL3A1, FGFR3, IGFBP6, CUL4B, HSPG2, GPC1, PTEN, HMGB1, SMAD2, MMP2, and CSGALNACT1) were selected for the following experiments (Fig. 1B). The expression of these 13 genes in IDD tissues and normal IVD tissues according to GSE34095 (Fig. 1C and D). The PCA analysis further confirmed these 13 genes could effectively classify the IDD and normal IVD groups in GSE34095 (Fig.S1).

3.2. Functional and disease-association analyses on 13 target genes

GO functional enrichment annotation and KEGG on 13 target genes performed using Metascape (https://metascape.org/gp/); we found the significant enrichment of these genes in AGE-RAGE signaling, proteoglycans in cancer, wound healing, transmembrane receptor protein tyrosine kinase signaling pathway, MAPK cascades, ERK1/2 cascades, PI3K/Akt signaling pathway, skeletal system, etc (Fig. 2A). Disease-association analysis on 13 target genes was performed using DisGeNET (https://www.disgenet.org/); these genes were significantly associated with IDD, intervertebral disc disease, skeletal dysplasia, and other diseases (Fig. 2B).

Next, the compound-target-signaling networks were constructed [20]. In these graphical networks, the chemicals, proteins, or pathways were represented by nodes, while the relationships between the substances, targets, or signaling were represented by edges (Fig. 3 and Table 2). As inferred from Fig. 3 and Table 2, among the 8 active compounds of DZ, only cyclopamine, quercetin, kaempferol and mairin could target 13 IDD disease genes that were enriched in 23 pathways (INTS8 did not have pathway enrichment; as a result, only 12 genes are shown in Fig. 3). Cyclopamine and mairin target 1 disease gene. Quercetin and kaempferol respectively target 11 and 2 disease genes. However, numerous studies have documented the role of quercetin in IDD [24,25]. The effect of kaempferol on NPCs has not yet been documented. Therefore, kaempferol has been considered the hub compound for further investigation.

3.3. Kaempferol improves IL-1β-induced NPC dysfunction

Next, the specific effects of kaempferol on IL-1β-induced NPC dysfunction were investigated. Procured NPCs were identified using Toluidine blue staining; Fig. 4A shows that the cytoplasm of NPCs was stained in purple-blue. In response to IL-1β stimulation (10 ng/ml, 24 h), aggrecan levels were significantly induced in NPCs as revealed by IF

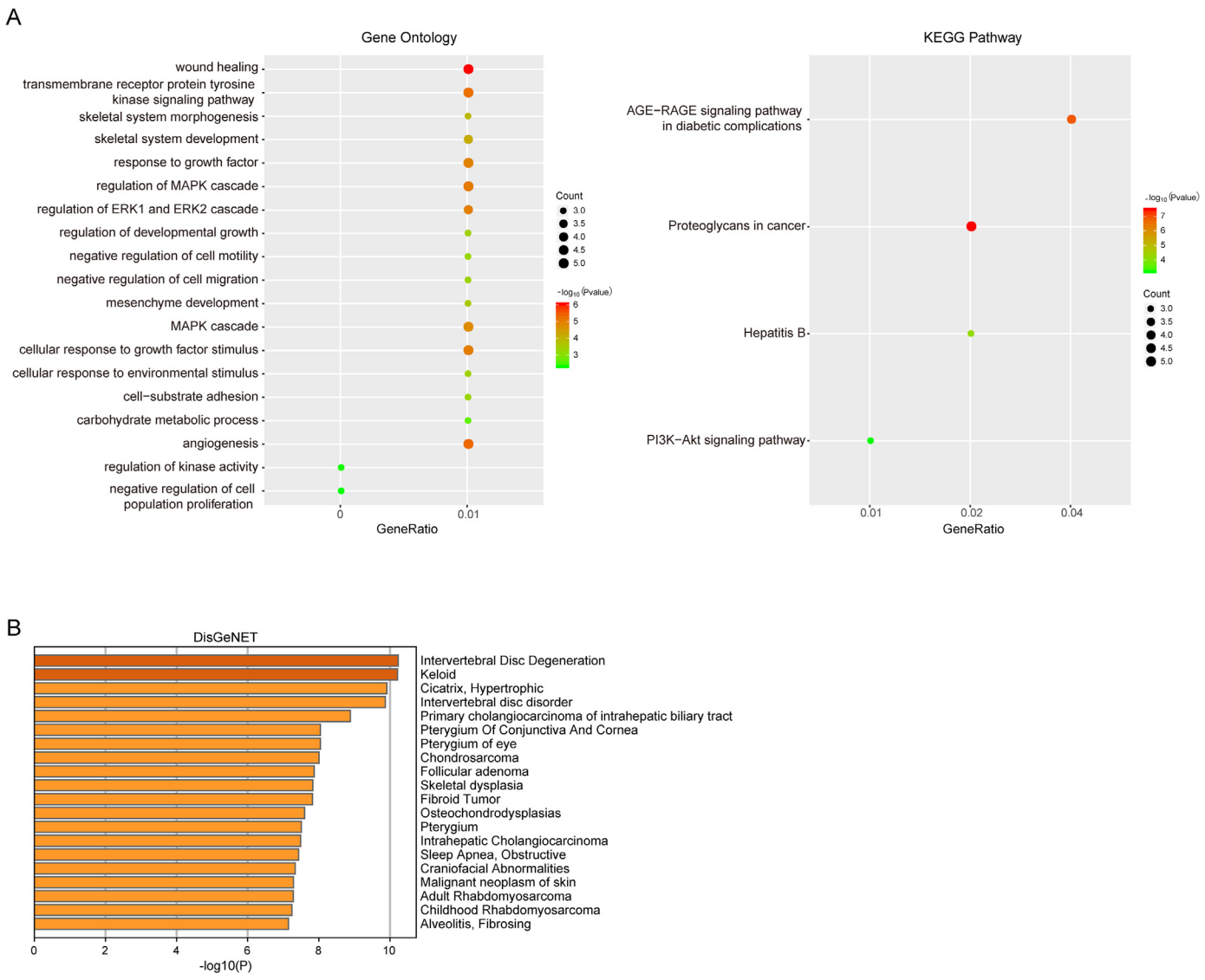

Fig 2. Functional and disease-association analyses on 13 target genes (A) Gene Ontology (GO) functional enrichment annotation and Kyoto Encyclopedia of Genes and Genomes (KEGG) enrichment analysis on the 13 target genes was performed using Metascape (https://metascape.org/gp/). The bubble charts were drawn by R language ggplot2 package (B) Disease-association analysis on 13 target genes was performed using DisGeNET (https://www.disgenet.org/).

staining (Fig. 4B). For selecting the minimum efficient dose of kaempferol, NPCs were treated with gradient concentrations of Kaempferol (0, 5, 10, 25, or 50 μM) and examined for cell viability; Fig. 4C shows that 10, 25, or 50 μM kaempferol significantly promoted NPC cell viability. Thus, 10 μM was selected for the following experiments. NPCs were exposed to IL-1β stimulation (10 ng/ml, 24 h), treated with 10 μM Kaempferol, and examined for related indexes. Regarding cell phenotypes, IL-1β stimulation remarkably suppressed cell viability (Fig. 4D) and promoted cell senescence (Fig. 4E); alterations in NPC viability and senescence induced by IL-1β were partially eliminated by kaempferol treatment (Fig. 4D and E). Furthermore, senescence-related factors were also examined. IL-1β stimulation significantly increased p16, p21, and Rb protein contents but decreased hTERT (Fig. 4F); similarly, IL-1β-induced alterations in senescence markers were partially eliminated by kaempferol treatment (Fig. 4F).

3.4. Kaempferol on oxidative damage and apoptosis of NPCs

IDD and oxidative stress are related. The primary risk factors for IDD have been identified as excessive ROS-induced senescence and apoptosis [26]. The levels of cellular ROS and the expression of genes associated with oxidative stress were assessed following exposure to IL-1β stimulation and kaempferol. Fig. 5A demonstrates that whereas kaempferol only marginally decreased the ROS level, IL-1β considerably increased the generation of ROS in NPCs. Results from qRT-PCR and immunoblotting revealed that IL- 1β stimulation reduced the mRNA and protein levels of the anti-oxidative factors Nrf2, HO-1, NQO-1, SOD1, and SOD2, but kaempferol only partially mitigated IL-1-β induced oxidative changes (Fig. 5B and C). The apoptotic cell rate was dramatically raised by IL- 1β, which also caused changes in the levels of the pro-apoptotic proteins Cleaved-caspase 3, Bax, and Bcl-2. Kaempferol partially reversed the effects of IL-1β on apoptosis, as shown in Fig. 5D–F. Bax and Bcl-2 mRNA levels were regulated by IL-1β and partially reversed by treatment with kaempferol (Fig. 5E).

3.5. Effects of kaempferol IL-1β-induced ECM deposition

Next, the specific effects of kaempferol on IL-1β-induced ECM deposition were investigated. NPCs were treated accordingly and evaluated for the protein levels of ECM production- and degradation-related

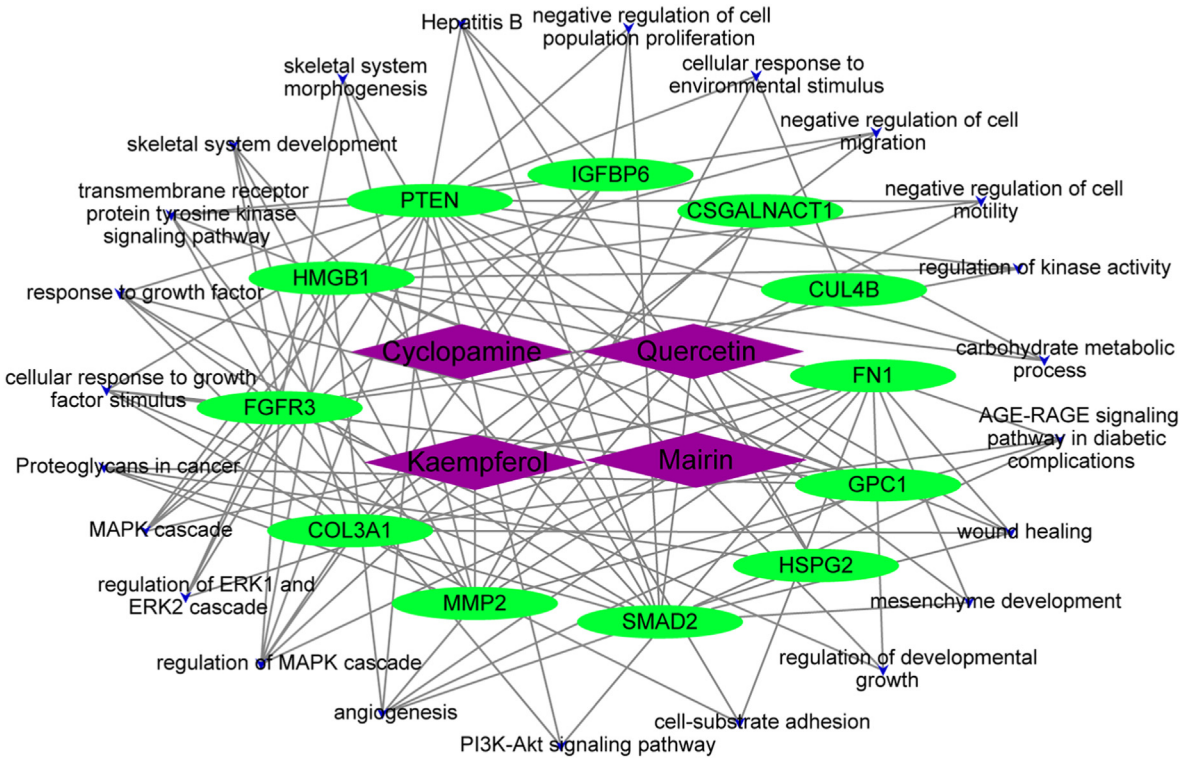

Fig 3. The compound-target-signaling networks generated using Cytoscape_v3.8.0. The active compounds cyclopamine, quercetin, kaempferol and mairin could target 12 IDD disease genes including HMGB1, PTEN, IGFBP6, FGFR3, COL3A1, MMP2, SMAD2, HSPG2, GPC1, FN1, CUL4B, CSGALNACT1 (Among 13 target genes, INTS8 did not have pathway enrichment). The compound-targeted disease genes were enriched in 23 pathways.

Table 2
Compound-target-signaling networks.

Compounds	protein	Pathway
Quercetin	FGFR3	skeletal system development, skeletal system morphogenesis, cellular response to growth factor stimulus, response to growth factor, regulation of developmental growth, PI3K-Akt signaling pathway, transmembrane receptor protein tyrosine kinase signaling pathway, regulation of MAPK cascade, regulation of ERK1 and ERK2 cascade, MAPK cascade, regulation of kinase activity
	FN1	Proteoglycans in cancer, AGE-RAGE signaling pathway in diabetic complications, wound healing, mesenchyme development, regulation of developmental growth, cell-substrate adhesion, PI3K-Akt signaling pathway, angiogenesis, regulation of MAPK cascade, regulation of ERK1 and ERK2 cascade, MAPK cascade
	GPC1	Proteoglycans in cancer, cellular response to growth factor stimulus, response to growth factor, angiogenesis, transmembrane receptor protein tyrosine kinase signaling pathway
	HMGB1	wound healing, angiogenesis, regulation of MAPK cascade, regulation of ERK1 and ERK2 cascade, MAPK cascade, negative regulation of cell migration, negative regulation of cell motility, carbohydrate metabolic process, regulation of kinase activity
	HSPG2	Proteoglycans in cancer, angiogenesis, Hepatitis B
	MMP2	Proteoglycans in cancer, AGE-RAGE signaling pathway in diabetic complications, skeletal system development, skeletal system morphogenesis, angiogenesis, transmembrane receptor protein tyrosine kinase signaling pathway, cellular response to environmental stimulus
	COL3A1	AGE-RAGE signaling pathway in diabetic complications, skeletal system development, wound healing, cellular response to growth factor stimulus, response to growth factor, cell-substrate adhesion, regulation of MAPK cascade, negative regulation of cell migration, negative regulation of cell motility
	CSGALNACT1	regulation of MAPK cascade, carbohydrate metabolic process
	CUL4B	cellular response to environmental stimulus
	PTEN	wound healing, cellular response to growth factor stimulus, response to growth factor, mesenchyme development, regulation of developmental growth, cell-substrate adhesion, PI3K-Akt signaling pathway, angiogenesis, transmembrane receptor protein tyrosine kinase signaling pathway, regulation of MAPK cascade, regulation of ERK1 and ERK2 cascade, MAPK cascade, negative regulation of cell migration, negative regulation of cell motility, carbohydrate metabolic process, regulation of kinase activity, Hepatitis B, negative regulation of cell population proliferation, cellular response to environmental stimulus
	SMAD2	keletal system development, skeletal system morphogenesis, wound healing, cellular response to growth factor stimulus, response to growth factor, mesenchyme development, Hepatitis B, negative regulation of cell population proliferation,
Kaempferol	FN1	Proteoglycans in cancer, AGE-RAGE signaling pathway in diabetic complications, wound healing, mesenchyme development, regulation of developmental growth, cell-substrate adhesion, PI3K-Akt signaling pathway, angiogenesis, regulation of MAPK cascade, regulation of ERK1 and ERK2 cascade, MAPK cascade
	MMP2	Proteoglycans in cancer, AGE-RAGE signaling pathway in diabetic complications, skeletal system development, skeletal system morphogenesis, angiogenesis, transmembrane receptor protein tyrosine kinase signaling pathway, cellular response to environmental stimulus
Mairin	MMP2	Proteoglycans in cancer, AGE-RAGE signaling pathway in diabetic complications, skeletal system development, skeletal system morphogenesis, angiogenesis, transmembrane receptor protein tyrosine kinase signaling pathway, cellular response to environmental stimulus
Cyclopamine	IGFBP6	transmembrane receptor protein tyrosine kinase signaling pathway, regulation of MAPK cascade, MAPK cascade, Hepatitis B, negative regulation of cell population proliferation

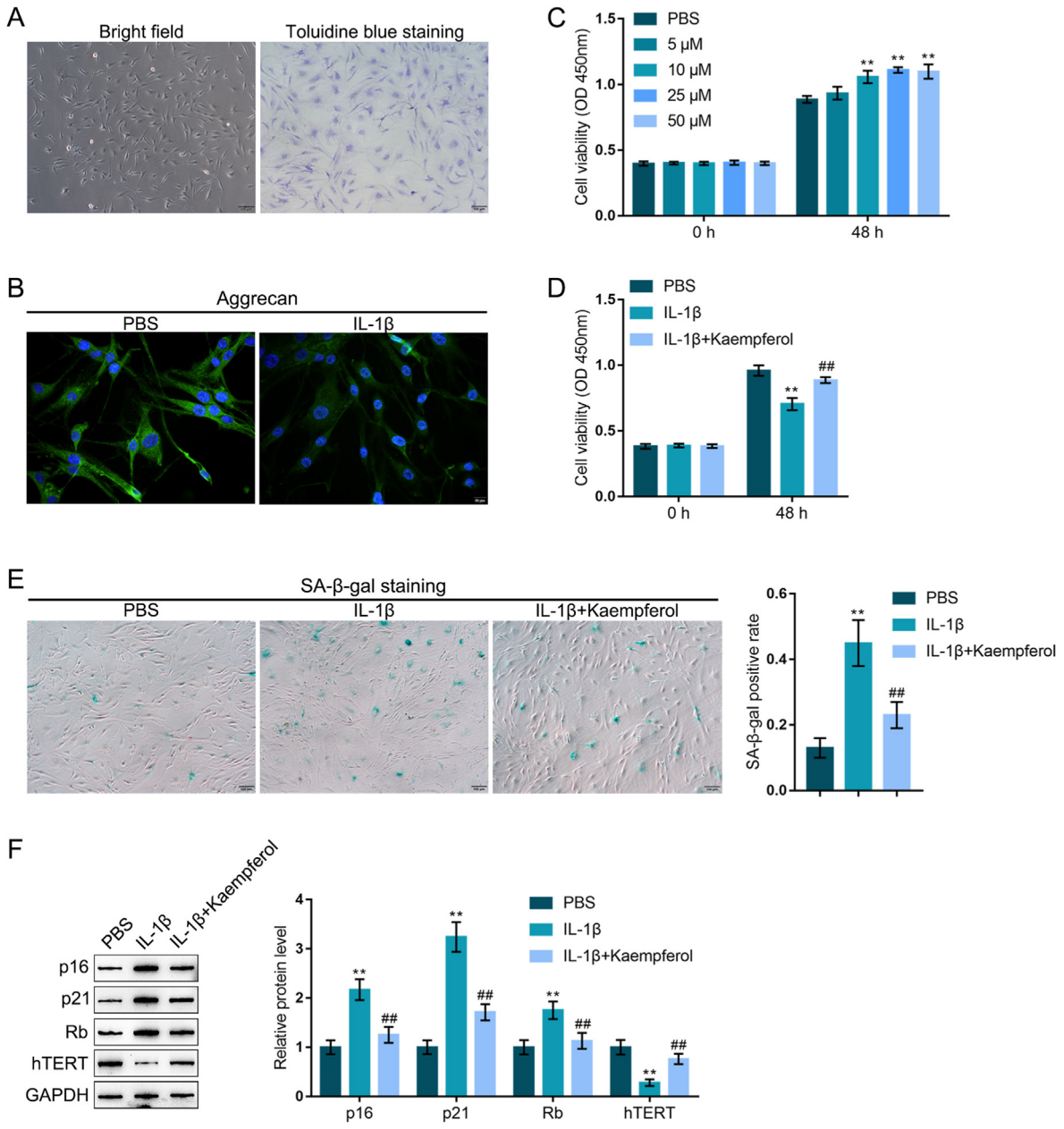

Fig 4. Kaempferol improves IL-1β-induced human nucleus pulposus cell (NPC) dysfunction (A) NPCs were identified using Toluidine blue staining (B) The levels of aggrecan in NPCs with or without IL-1β stimulation (10 ng/ml, 24 h) were examined using Immunofluorescent (IF) staining (C) NPCs were treated with gradient concentrations of kaempferol (0, 5, 10, 25, or 50 μM) and examined for cell viability using CCK-8 assay; 10 μM kaempferol was selected for the following experiments. Then, NPCs were exposed to IL-1β stimulation (10 ng/ml, 24 h), treated with 10 μM kaempferol, and examined for cell viability using CCK-8 assay (D); cell senescence using senescence-associated β-gal staining (E); the protein levels of p16, p21, Rb, and hTERT using Immunoblotting (F). N = 3, one-way ANOVA followed by Tukey's post hoc test. **p < 0.01, compared to PBS group; ##p < 0.01, compared with IL-1β group.

factors. Fig. 6A–D shows that IL-1β significantly decreased aggrecan, collagen II, SOX9, and FN1 mRNA and protein levels, whereas increased MMP3, MMP13, ADAMTS-4, and ADAMTS-5 mRNA and protein levels; IL-1β-induced alterations in ECM production- and degradation-related factors were partially abolished by kaempferol treatment (Fig. 6A–D).

3.6. *Effects of kaempferol on IL-1β-induced MAPK signaling pathway activation*

Finally, since the 12 target genes were shown to be linked to the MAPK, ERK, and PI3K/Akt pathways (Fig. 3), and MAPK signaling pathway has been widely reported as a potential target for the treatment of IDD [27,28], the effects of kaempferol IL-1β-caused MAPK pathway activation were investigated. NPCs were treated accordingly and examined for p-p38, p38, p-JNK, JNK, p-ERK1/2, and ERK1/2 protein contents. Fig. 7A shows that IL-1β dramatically enhanced p38, JNK, and ERK1/2 phosphorylation, while kaempferol treatment significantly relieved the promotive effects of IL-1β stimulation upon p38, JNK, and ERK1/2 phosphorylation. Next, the ERK1/2 inhibitor PD0325901 was used to confirm the function of kaempferol. As is shown in Fig. 7B, under IL-1β stimulation, ERK1/2 inhibition also prevented ERK1/2 phosphorylation. The effects of ERK1/2 inhibitor further increased the effects of kaempferol in downregulating MMP3 and ADAMTS-4 expression and upregulating aggrecan and collagen II expressions.

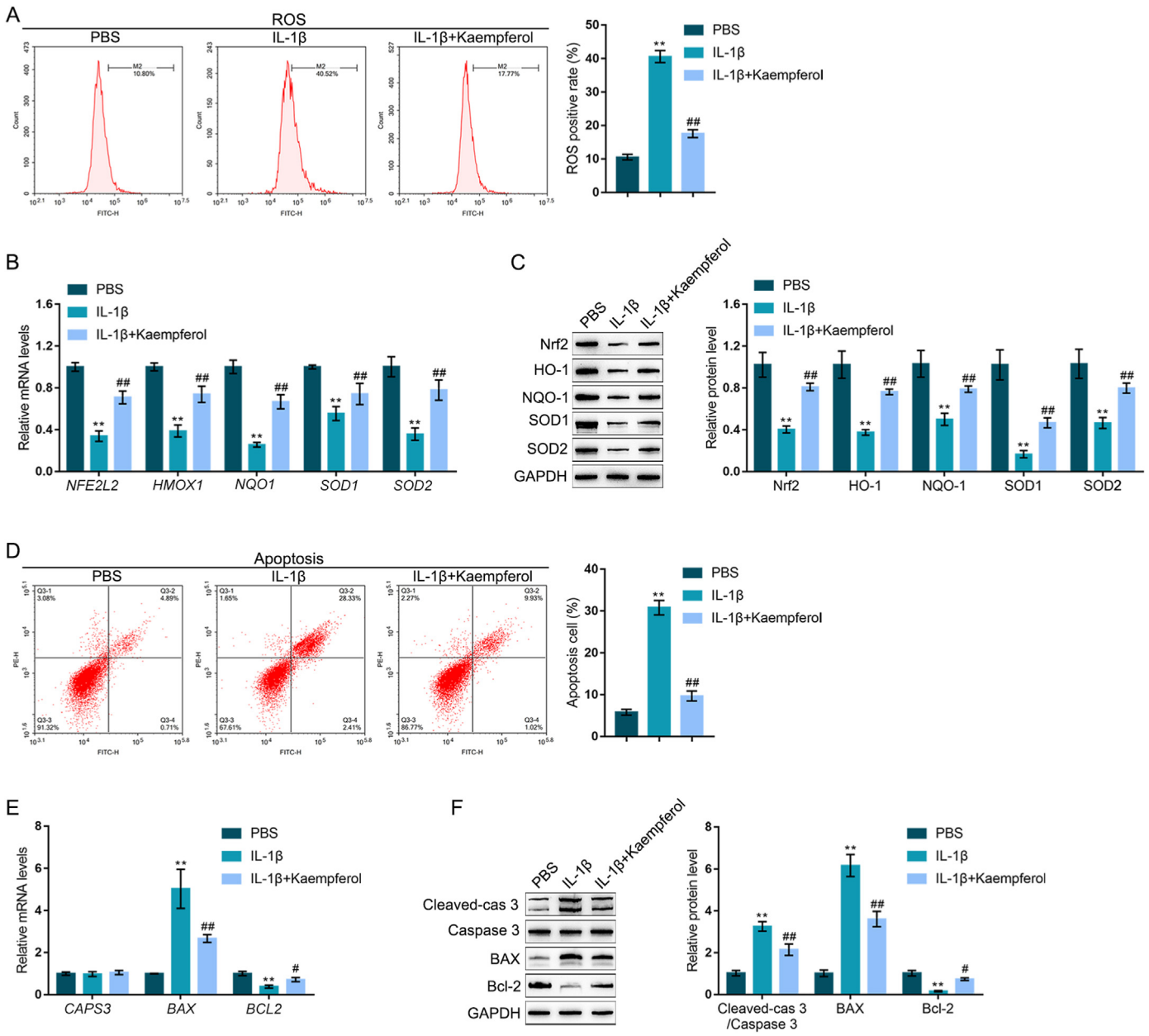

Fig 5. Effects of kaempferol on oxidative damage and apoptosis of NPCs were exposed to IL-1β stimulation (10 ng/ml, 24 h), treated with 10 μM kaempferol, and examined for ROS and apoptosis with flow cytometry assay and Immunoblotting (A) ROS level in cells (B–C) The mRNA and protein levels of Nrf2, HO-1, NQO-1, SOD1 and SOD2 were examined (D) The apoptosis rate of NPCs was determined by the FITC-Anexin-V/PI apoptosis assay kit. The cells with Annexin-V positive/PI negative and Annexin-V positive/PI positive were considered apoptotic cells (E) The mRNA levels of caspase-3, Bax and Bcl-2 were examined (F) The protein levels of Cleaved-caspase 3, Caspase 3, Bax, and Bcl-2 were examined. One-way ANOVA followed by Tukey's post hoc test. N = 3, **p < 0.01, compared to PBS group; #p < 0.05, ##p < 0.01, compared with IL-1β group.

4. Discussion

Herein, the main active compounds of DZ were retrieved from TCMSP and 8 of them were found to meet the threshold of OB ≥ 30% and DL ≥ 0.2. Among 4151 drug targets, 879 disease targets, and 230 DEGs, 13 hub genes overlapped. According to functional enrichment annotation and disease association analyses, these genes showed to be dramatically enriched in AGE-RAGE signaling, proteoglycans in cancer, wound healing, transmembrane receptor protein tyrosine kinase signaling, MAPK cascades, ERK1/2 cascades, PI3K/Akt signaling pathway, skeletal system, etc. DisGeNET analysis indicated that these genes were significantly associated with IDD, intervertebral disc disease, skeletal dysplasia and other diseases. Networks of active components, targets, and signaling pathways were built, and kaempferol was shown to be the central active constituent. Treatment with kaempferol greatly reduced the induction of senescence, oxidative stress, apoptosis, and viability decrease in NPC cells caused by IL-1β. Additionally, IL-1-induced elevations in MMP3, MMP13, ADAMTS-4, ADAMTS-5, and pro-apoptotic gene expression and decreases in aggrecan, collagen II, SOX9, FN1, anti-oxidative, and anti-apoptotic gene levels were partially reversed by kaempferol administration. Additionally, kaempferol therapy dramatically reduced the stimulatory effects of IL-1β activation on the phosphorylation of p38, JNK, and ERK1/2.

The majority of the chemical elements in DZ have theoretically and clinically demonstrated pharmacological efficacies. DZ is a supplier of pharmaceuticals and healthcare products with a wide range of

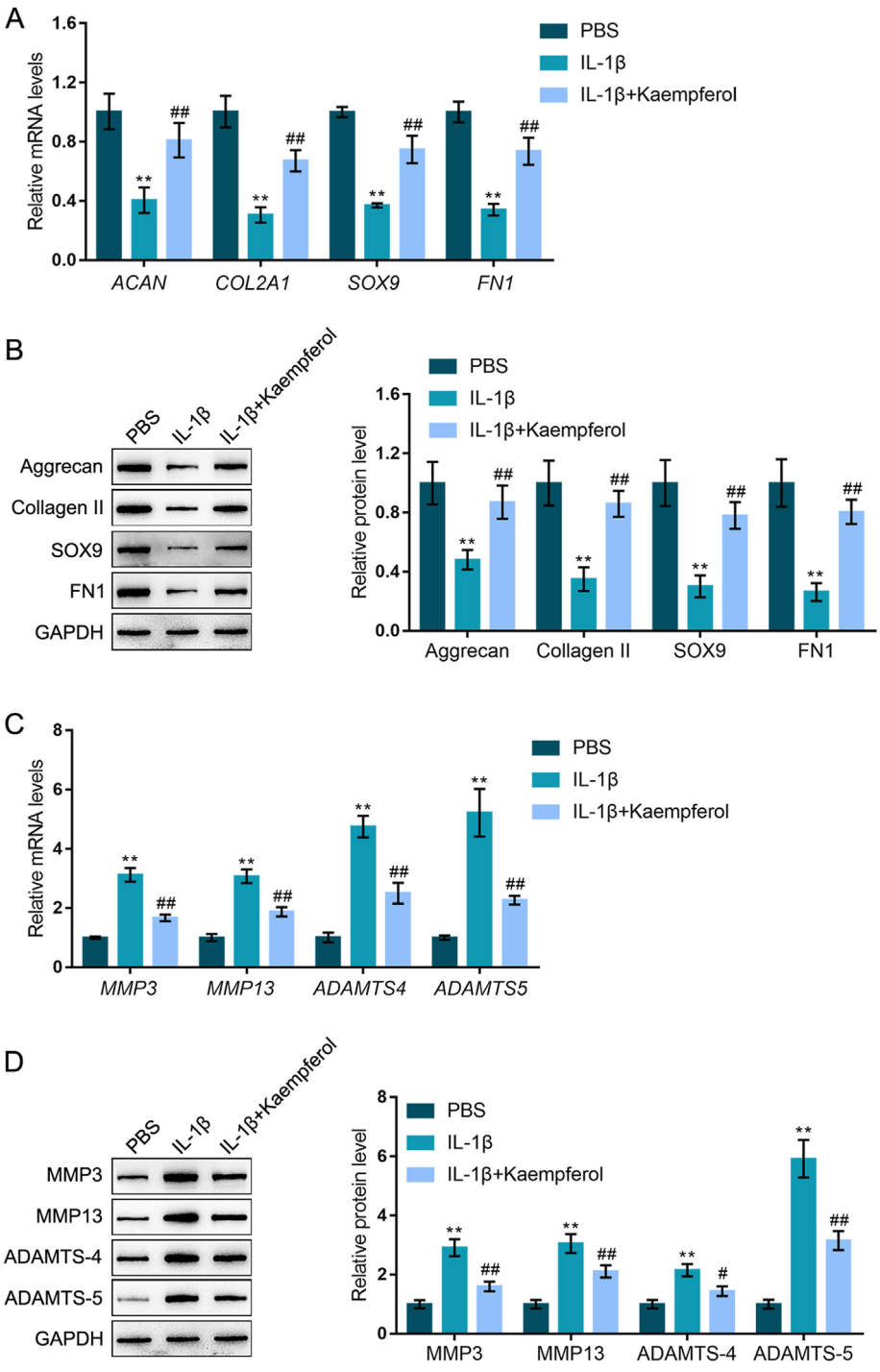

Fig. 6. Effects of Kaempferol IL-1β-induced ECM deposition NPCs were exposed to IL-1β stimulation (10 ng/ml, 24 h), treated with 10 μM kaempferol, and examined for the mRNA and protein levels of aggrecan, collagen II, SOX9, FN1 (A–B), MMP3, MMP13, ADAMTS-4, and ADAMTS-5 (C–D) using qRT-PCR and Immunoblotting, respectively. . One-way ANOVA followed by Tukey's post hoc test. N = 3, **p < 0.01, compared to PBS group; #p < 0.05, ##p < 0.01, compared with IL-1β group.

pharmacological effects, non-toxic properties, and minimal side effects [29]. The pharmacological effects of DZ's functional components include protective effects for the heart, liver, kidney, lung, and bone as well as anti-hypertensive, hypolipidemic, hypoglycemia, anti-inflammatory, antioxidative, anti-tumor, anti-bacterial, and anti-viral qualities [30]. According to reports, DZ and its active components are frequently employed in IDD treatment plans. A TCM formula called Bu-Shen-Huo-Xue-Fang that contains DZ can encourage NP cell proliferation and ECM synthesis [31]. One of the DZ active ingredients, aucubin, has properties that protect the chondrocytes and have anti-inflammatory, anti-oxidant, and osteogenic effects [32]. In this study, a total of 8 active compounds of DZ were collected from TCMSP using the thresholds of OB ≥ 30%, DL ≥ 0.2, including ent-Epicatechin, β-sitosterol, Cyclopamine, Acanthoside B, quercetin, β-carotene, kaempferol, and Mairin.

The antioxidant, anti-inflammatory, and anti-aging effects of ent-Epicatechin have been reported previously [33]. β-Sitosterol also exerts anti-inflammatory activity in bone diseases [34]. Regarding cyclopamine, applying cyclopamine to inhibit Indian hedgehog was effective in preventing NPC apoptosis without decreasing ROS level [35].

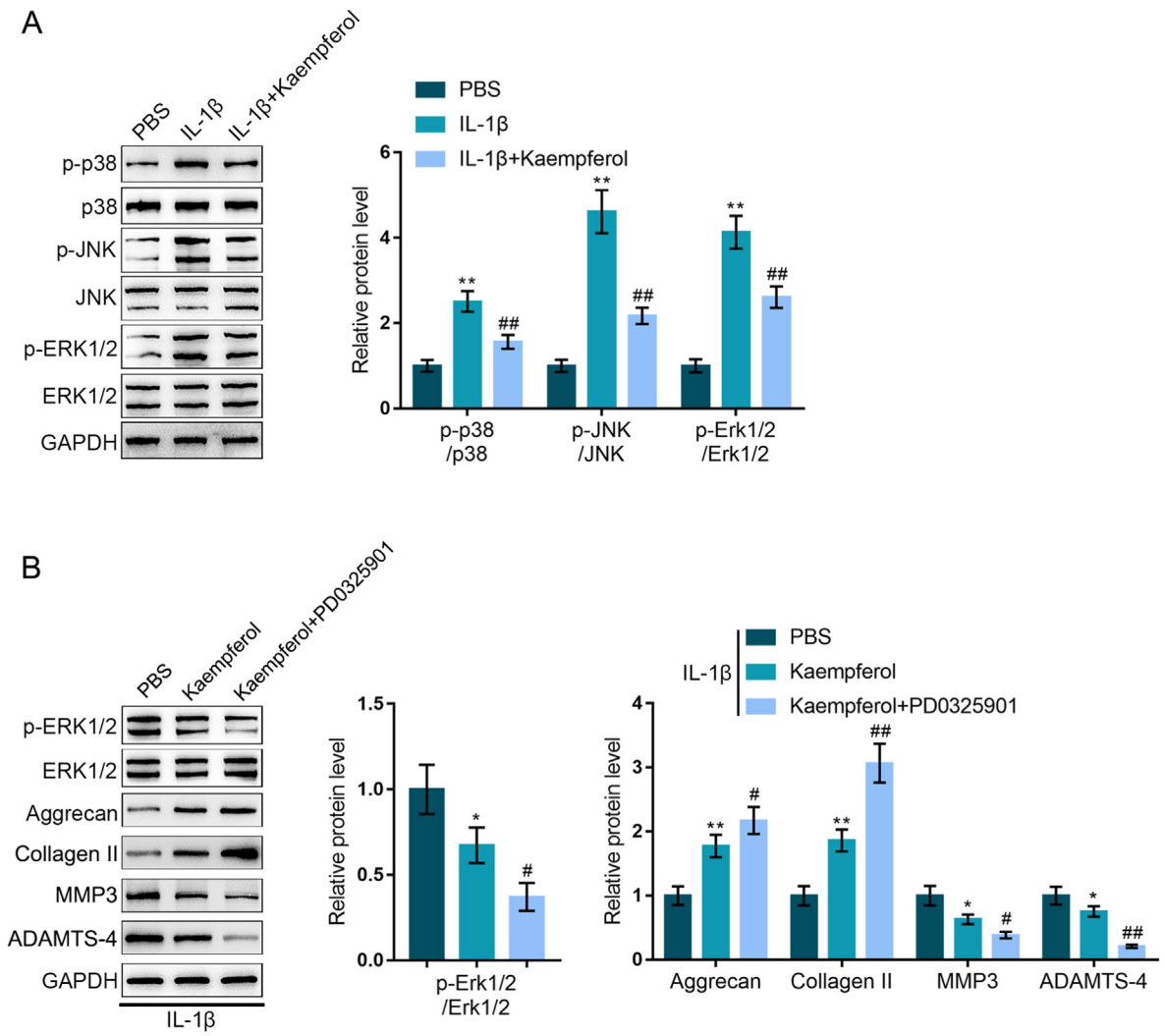

Fig. 7. Effects of Kaempferol on IL-1β-induced MAPK signaling pathway activation (A) NPCs were exposed to IL-1β stimulation (10 ng/ml, 24 h), treated with 10 μM kaempferol, and examined for the protein levels of p-p38, p38, p-JNK, JNK, p-ERK1/2, and ERK1/2 using Immunoblotting (B) Under IL-1β stimulation, NPCs were co-treated with 10 μM kaempferol and 1 μM PD0325901, and examined for the protein levels of aggrecan, collagen II, MMP3 and ADAMTS-4 using immunoblotting. One-way ANOVA followed by Tukey's post hoc test. N = 3, *p < 0.05, **p < 0.01, compared to PBS group; #p < 0.05, ##p < 0.01, compared with IL-1β group or kaempferol group.

Acanthoside B has been demonstrated to have an anti-inflammatory effect in LPS-stimulated RAW 264.7 macrophage cells or lung inflammation, but not directly in bone disorders [36]. Quercetin could ameliorate IDD [25]. β-carotene could prevent bone loss and bone resorption [37]. Kaempferol inhibits IVD degeneration through altering the LPS-mediated imbalance between osteogenesis and adipogenesis and inflammatory response in bone marrow-derived mesenchymal stem cells (BMSCs) [38]. Mairin might be associated with inflammatory target genes in rheumatoid arthritis [39]. Unknown, however, are the fundamental active elements and hub-genes that control DZ defense against IDD as well as the underlying mechanism.

13 hub genes were found to overlap among 4151 pharmacological targets, 879 disease targets, and 230 DEGs by studies of the GeneCards and GEO expression profiles. Usually, the fold change threshold for DEGs screening in GSE datasets is |logFC|>1. However, in the present study, the result of |logFC|>1 threshold can only screen out one different DZ drug target gene in GSE34095. In order to better explore the application value of the DZ drug target gene in IDD, we appropriately relaxed the screening threshold to |logFC|>0.3, which is acceptable in other research [40,41]. Thirteen drug-target gene DEGs were identified. According to functional enrichment annotation analysis of these genes analyses, we found a significant enrichment in AGE-RAGE signaling [42], proteoglycans [43,44], wound healing, transmembrane receptor protein tyrosine kinase signaling pathway, MAPK cascades [27,45], ERK1/2 cascades [27,45], PI3K/Akt signaling pathway [46], skeletal system, etc.; reportedly, these signaling pathways or processes play a critical role in IDD progression. These genes were found to be strongly related to IDD, intervertebral disc disease, skeletal dysplasia, and other disorders, according to a DisGeNET analysis. Networks of active components, targets, and signaling pathways were built, and kaempferol was shown to be the central active constituent. As indicated earlier, kaempferol has been shown to reduce the imbalance between osteogenesis and adipogenesis and the inflammatory response in BMSCs, which is induced by LPS [38]; however, its specific effects on NPCs remain unclear.

As previously reported, IL-1β plays a role in eliciting NPC apoptosis, oxidative stress, and senescence [27,28]. Furthermore, NPCs in the intervertebral disc exert a pivotal effect on the maintenance of ECM homeostasis [34]. The NP ECM is predominantly composed of proteoglycans (mostly aggrecan) and type II collagen, which contribute to maintaining IVD physiological activities [34,35]. MMPs have been reported to be essential enzymes for collagen/aggrecan cleavage in NP ECM; MMP up-regulation has been found to result in ECM degradation

and IDD development [36]. Reduced ECM function, elevated synthesis of degradative enzymes, and upregulated expression of inflammatory cytokines lead to the loss of structural integrity and acceleration in IDD [37]. The metabolism and ECM structure were both susceptible to oxidative stress. Oxidative stress may cause cell death and senescence in disc cells in addition to disrupting the ECM in these cells [26]. The antioxidant role of kaempferol has been reported in various cell types, including epithelial cells [47], neuronal cells [48] and cardiomyocytes [49]. In this study, IL-1β-induced NP cell viability suppression, ECM degradation, NP cell senescence, Oxidative stress and cell apoptosis, could be reversed by kaempferol. These findings indicated that kaempferol's anti-oxidative properties contributed to its preventive impact in IDD.

Numerous studies have reported that activation of the MAPK signal pathway can accelerate ECM degradation via increasing MMP production and ADAMTS-5 expression during the IDD process [50,51]. Moreover, inhibition of the MAPK signal pathway is a potential strategy against inflammation-induced apoptosis, senescence and oxidative stress in IVD cells [52,53]. In rheumatoid arthritis synovial fibroblasts and chondrocytes, kaempferol could inhibit IL-1β-induced production of MMPs and phosphorylation of ERK and p38 [54]. Herein, kaempferol also blocked IL-1β-induced activation of MAPK pathway. The ECM degradation-related genes were further decreased by the ERK inhibitor.

Conclusively, through network pharmacology-based integrative bioinformatics analyses, kaempferol has been regarded as the major active compound of DZ, protecting NPCs from IL-1β-induced damages through promoting cell viability, inhibiting cell senescence, apoptosis, and oxidative stress, increasing ECM production, and decreasing ECM degradation. However, there may be limitations to this study. We solely looked into how kaempferol affected the MAPK signaling pathway and cellular phenotype in NPCs. Further research is required to determine and understand the precise pharmacological target of kaempferol. Another restriction is a paucity of *in vivo* data. It is necessary to confirm the roles of kaempferol in animal models of IDD.

Declaration of competing interest

All the authors declare that they have no conflicts of interest in this work.

Acknowledgments

This study was supported by the National Natural Science Foundation of China (Grant No. 81871821) and the Natural Science Foundation of Hunan Province, China (Grant No. 2021JJ30958; No. 2021JJ30952).

Appendix A. Supplementary data

Supplementary data related to this article can be found at https://doi.org/10.1016/j.jot.2023.01.002.

Table S1 The primers for qRT-PCR

Gene name	F	R
NFE2L2	TCAGCGACGGAAAGAGTATGA	CCACTGGTTTCTGACTGGATGT
HMOX1	AAGACTGCGTTCCTGCTCAAC	AAAGCCCTACAGCAACTGTCG
NQO1	GAAGAGCACTGATCGTACTGGC	GGATACTGAAAGTTCGCAGGG
SOD1	GGTGGGCCAAAGGATGAAGAG	CCACAAGCCAAACGACTTCC
SOD2	GCTCCGGTTTTGGGGTATCTG	GCGTTGATGTGAGGTTCCAG
GAPDH	ACAGCCTCAAGATCATCAGC	GGTCATGAGTCCTTCCACGAT
CAPS3	AGAGGGGATCGTTGTAGAAGTC	ACAGTCCAGTTCTGTACCACG
BAX	CCCGAGAGGTCTTTTTCCGAG	CCAGCCCATGATGGTTCTGAT
BCL2	GGTGGGGTCATGTGTGTGG	CGGTTCAGGTACTCAGTCATCC
ACAN	GTGCCTATCAGGACAAGGTCT	GATGCCTTTCACCACGACTTC
COL2A1	TGGACGCCATGAAGGTTTTCT	TGGGAGCCAGATTGTCATCTC
SOX9	AGCGAACGCACATCAAGAC	CTGTAGGCGATCTGTTGGGG
FN1	CGGTGGCTGTCAGTCAAAG	AAACCTCGGCTTCCTCCATAA

References

[1] Priyadarshani P, Li Y, Yao L. Advances in biological therapy for nucleus pulposus regeneration. Osteoarthritis Cartilage 2016;24(2):206–12.
[2] Verfaillie T, Garg AD, Agostinis P. Targeting ER stress induced apoptosis and inflammation in cancer. Cancer Lett 2013;332(2):249–64.
[3] Vergroesen PP, Kingma I, Emanuel KS, Hoogendoorn RJ, Welting TJ, van Royen BJ, et al. Mechanics and biology in intervertebral disc degeneration: a vicious circle. Osteoarthritis Cartilage 2015;23(7):1057–70.
[4] Yang W, Yu XH, Wang C, He WS, Zhang SJ, Yan YG, et al. Interleukin-1β in intervertebral disk degeneration. Clinica chimica acta; international journal of clinical chemistry 2015;450:262–72 [eng].
[5] Setty AR, Sigal LH. Herbal medications commonly used in the practice of rheumatology: mechanisms of action, efficacy, and side effects. Semin Arthritis Rheum 2005;34(6):773–84.
[6] Hou W, Liu B, Xu H. Celastrol: progresses in structure-modifications, structure-activity relationships, pharmacology and toxicology. Eur J Med Chem 2020;189:112081.
[7] Kim CH, Chung CK, Park CS, Choi B, Kim MJ, Park BJ. Reoperation rate after surgery for lumbar herniated intervertebral disc disease: nationwide cohort study. Spine 2013;38(7):581–90.
[8] Delgado-López PD, Rodríguez-Salazar A, Martín-Alonso J, Martín-Velasco V. Lumbar disc herniation: Natural history, role of physical examination, timing of surgery, treatment options and conflicts of interests. Neurocirugia 2017;28(3):124–34.
[9] Zhu L, Yu C, Zhang X, Yu Z, Zhan F, Yu X, et al. The treatment of intervertebral disc degeneration using Traditional Chinese Medicine. J Ethnopharmacol 2020;263:113117.
[10] Dai S, Shi X, Qin R, Zhang X, Xu F, Yang H. Sodium tanshinone IIA sulfonate ameliorates injury-induced oxidative stress and intervertebral disc degeneration in rats by inhibiting p38 MAPK signaling pathway. Oxid Med Cell Longev 2021;2021:5556122 [eng].
[11] Yang S, Li L, Zhu L, Zhang C, Li Z, Guo Y, et al. Aucubin inhibits IL-1beta- or TNF-alpha-induced extracellular matrix degradation in nucleus pulposus cell through blocking the miR-140-5p/CREB1 axis. J Cell Physiol 2019;234(8):13639–48.
[12] Hopkins AL. Network pharmacology: the next paradigm in drug discovery. Nat Chem Biol 2008;4(11):682–90.
[13] Jiao X, Jin X, Ma Y, Yang Y, Li J, Liang L, et al. A comprehensive application: molecular docking and network pharmacology for the prediction of bioactive constituents and elucidation of mechanisms of action in component-based Chinese medicine. Comput Biol Chem 2021;90:107402.
[14] Ru J, Li P, Wang J, Zhou W, Li B, Huang C, et al. TCMSP: a database of systems pharmacology for drug discovery from herbal medicines. J Cheminf 2014;6:13.
[15] Jia CY, Li JY, Hao GF, Yang GF. A drug-likeness toolbox facilitates ADMET study in drug discovery. Drug Discov Today 2020;25(1):248–58.
[16] Tang Y, Wang S, Liu Y, Wang X. Microarray analysis of genes and gene functions in disc degeneration. Exp Ther Med 2014;7(2):343–8 [eng].
[17] Davis S, Meltzer PS. GEOquery: a bridge between the gene expression Omnibus (GEO) and BioConductor. Bioinformatics 2007;23(14):1846–7 [eng].
[18] Zhou Y, Zhou B, Pache L, Chang M, Khodabakhshi AH, Tanaseichuk O, et al. Metascape provides a biologist-oriented resource for the analysis of systems-level datasets. Nat Commun 2019;10(1):1523.

[19] Pinero J, Sauch J, Sanz F, Furlong LI. The DisGeNET cytoscape app: exploring and visualizing disease genomics data. Comput Struct Biotechnol J 2021;19:2960–7.
[20] Smoot ME, Ono K, Ruscheinski J, Wang PL, Ideker T. Cytoscape 2.8: new features for data integration and network visualization. Bioinformatics 2011;27(3):431–2.
[21] Wang X, Li D, Wu H, Liu F, Liu F, Zhang Q, et al. LncRNA TRPC7-AS1 regulates nucleus pulposus cellular senescence and ECM synthesis via competing with HPN for miR-4769-5p binding. Mechanisms of ageing and development 2020;190:111293 [eng].
[22] Chen J, Jia YS, Liu GZ, Sun Q, Zhang F, Ma S, et al. Role of LncRNA TUG1 in intervertebral disc degeneration and nucleus pulposus cells via regulating Wnt/beta-catenin signaling pathway. Biochem Biophys Res Commun 2017;491(3):668–74.
[23] Livak KJ, Schmittgen TD. Analysis of relative gene expression data using real-time quantitative PCR and the 2− ΔΔCT method. Methods (Orlando) 2001;25(4):402–8.
[24] Wang D, He X, Wang D, Peng P, Xu X, Gao B, et al. Quercetin suppresses apoptosis and attenuates intervertebral disc degeneration via the SIRT1-autophagy pathway. Front Cell Dev Biol 2020;8:613006.
[25] Zhang S, Liang W, Abulizi Y, Xu T, Cao R, Xun C, et al. Quercetin alleviates intervertebral disc degeneration by modulating p38 MAPK-mediated autophagy. BioMed Res Int 2021;2021:6631562.
[26] Feng C, Yang M, Lan M, Liu C, Zhang Y, Huang B, et al. ROS: crucial intermediators in the pathogenesis of intervertebral disc degeneration. Oxid Med Cell Longev 2017. 2017:5601593.
[27] Zhang HJ, Liao HY, Bai DY, Wang ZQ, Xie XW. MAPK/ERK signaling pathway: a potential target for the treatment of intervertebral disc degeneration. Biomed Pharmacother 2021;143:112170.
[28] Studer RK, Aboka AM, Gilbertson LG, Georgescu H, Sowa G, Vo N, et al. p38 MAPK inhibition in nucleus pulposus cells: a potential target for treating intervertebral disc degeneration. Spine 2007;32(25):2827–33.
[29] Wang CY, Tang L, Li L, Zhou Q, Li YJ, Li J, et al. Geographic authentication of Eucommia ulmoides leaves using multivariate analysis and preliminary study on the compositional response to environment. Front Plant Sci 2020;11:79.
[30] Wang CY, Tang L, He JW, Li J, Wang YZ. Ethnobotany, phytochemistry and pharmacological properties of Eucommia ulmoides: a review. Am J Chin Med 2019;47(2):259–300.
[31] Yang S, Li L, Zhu L, Zhang C, Li Z, Guo Y, et al. Bu-Shen-Huo-Xue-Fang modulates nucleus pulposus cell proliferation and extracellular matrix remodeling in intervertebral disk degeneration through miR-483 regulation of Wnt pathway. J Cell Biochem 2019;120(12):19318–29.
[32] Young IC, Chuang ST, Hsu CH, Sun YJ, Liu HC, Chen YS, et al. Protective effects of aucubin on osteoarthritic chondrocyte model induced by hydrogen peroxide and mechanical stimulus. BMC Compl Alternative Med 2017;17(1):91.
[33] Grenier A, Legault J, Pichette A, Jean L, Belanger A, Pouliot R. Antioxidant, anti-inflammatory, and anti-aging potential of a kalmia angustifolia extract and identification of some major compounds. Antioxidants 2021;10(9):1373.
[34] Liu R, Hao D, Xu W, Li J, Li X, Shen D, et al. beta-Sitosterol modulates macrophage polarization and attenuates rheumatoid inflammation in mice. Pharm Biol 2019;57(1):161–8.
[35] Bao J, Qian Z, Liu L, Hong X, Che H, Wu X. Pharmacological disruption of phosphorylated eukaryotic initiation factor-2alpha/activating transcription factor 4/Indian hedgehog protects intervertebral disc degeneration via reducing the reactive oxygen species and apoptosis of nucleus pulposus cells. Front Cell Dev Biol 2021;9:675486.
[36] Lee JH, Sun YN, Kim YH, Lee SK, Kim HP. Inhibition of lung inflammation by acanthopanax divaricatus var. Albeofructus and its constituents. Biomol Ther (Seoul) 2016;24(1):67–74.
[37] Matsumoto Y, Tousen Y, Ishimi Y. beta-Carotene prevents bone loss in hind limb unloading mice. J Clin Biochem Nutr 2018;63(1):42–9.
[38] Zhu J, Tang H, Zhang Z, Zhang Y, Qiu C, Zhang L, et al. Kaempferol slows intervertebral disc degeneration by modifying LPS-induced osteogenesis/adipogenesis imbalance and inflammation response in BMSCs. Int Immunopharm 2017;43:236–42.
[39] Bai LL, Chen H, Zhou P, Yu J. Identification of tumor necrosis factor-alpha (TNF-alpha) inhibitor in rheumatoid arthritis using network pharmacology and molecular docking. Front Pharmacol 2021;12:690118.
[40] Xing M, Shi J, Li P, Qin J, Zhang X, Ma Y, et al. Abstract 4591: overexpression of p62/IMP2 can promote cell migration in hepatocellular carcinoma (HCC) via activating Wnt/β-catenin pathway. Cancer Res 2019;79(13_Supplement). 4591-91.
[41] Izzo A, Manco R, Bonfiglio F, Calì G, De Cristofaro T, Patergnani S, et al. NRIP1/RIP140 siRNA-mediated attenuation counteracts mitochondrial dysfunction in Down syndrome. Hum Mol Genet 2014;23(16):4406–19.
[42] Xia B, Xing J, Ai Q, Li H, Xu M, Hou T. [Expression profile of intervertebral disc degeneration-specific genes: a transcriptome sequencing-based analysis]. Nan Fang Yi Ke Da Xue Xue Bao 2021;41(6):883–90.
[43] Xu X, Wang D, Zheng C, Gao B, Fan J, Cheng P, et al. Progerin accumulation in nucleus pulposus cells impairs mitochondrial function and induces intervertebral disc degeneration and therapeutic effects of sulforaphane. Theranostics 2019;9(8):2252–67.
[44] Vadala G, Russo F, Ambrosio L, Papalia R, Denaro V. Mesenchymal stem cells for intervertebral disc regeneration. J Biol Regul Homeost Agents 2016;30(4 Suppl 1):173–9.
[45] Studer RK, Aboka AM, Gilbertson LG, Georgescu H, Sowa G, Vo N, et al. p38 MAPK inhibition in nucleus pulposus cells: a potential target for treating intervertebral disc degeneration. Spine (Phila Pa 1976 2007;32(25):2827–33.
[46] Ouyang ZH, Wang WJ, Yan YG, Wang B, Lv GH. The PI3K/Akt pathway: a critical player in intervertebral disc degeneration. Oncotarget 2017;8(34):57870–81.
[47] Du W, An Y, He X, Zhang D, He W. Protection of kaempferol on oxidative stress-induced retinal pigment epithelial cell damage. Oxid Med Cell Longev 2018. 2018:1610751.
[48] Yang E-J, Kim G-S, Jun M, Song K-S. Kaempferol attenuates the glutamate-induced oxidative stress in mouse-derived hippocampal neuronal HT22 cells. Food Funct 2014;5(7):1395–402.
[49] Du Y, Han J, Zhang H, Xu J, Jiang L, Ge W. Kaempferol prevents against Ang II-induced cardiac remodeling through attenuating Ang II-induced inflammation and oxidative stress. J Cardiovasc Pharmacol 2019;74(4):326.
[50] Liu C, Yang H, Gao F, Li X, An Y, Wang J, et al. Resistin promotes intervertebral disc degeneration by upregulation of ADAMTS-5 through p38 MAPK signaling pathway. Spine 2016;41(18):1414–20 [eng].
[51] Zhang J, Li Z, Chen F, Liu H, Wang H, Li X, et al. TGF-β1 suppresses CCL3/4 expression through the ERK signaling pathway and inhibits intervertebral disc degeneration and inflammation-related pain in a rat model. Exp Mol Med 2017;49(9):e379 [eng].
[52] Chen Z, Liu M, Zhang W, Deng M, Zhou Y, Li Y. miR-24-3p induces human intervertebral disc degeneration by targeting insulin-like growth factor binding protein 5 and the ERK signaling pathway. Life Sci 2020;243:117288 [eng].
[53] Chen Z, Yu Y, Wa Q, Zhou J, He M, Cen Y. The role of quinazoline in ameliorating intervertebral disc degeneration by inhibiting oxidative stress and anti-inflammation via NF-κB/MAPKs signaling pathway. Eur Rev Med Pharmacol Sci 2020;24(4):2077–86.
[54] Yoon HY, Lee EG, Lee H, Cho IJ, Choi YJ, Sung MS, et al. Kaempferol inhibits IL-1β-induced proliferation of rheumatoid arthritis synovial fibroblasts and the production of COX-2, PGE2 and MMPs. Int J Mol Med 2013;32(4):971–7 [eng].